DISTRIBUTED SOURCE LOCALIZATION WITH MULTIPLE SENSOR ARRAYS AND FREQUENCY-SELECTIVE SPATIAL COHERENCE

Richard J. Kozick

Bucknell University
Lewisburg, PA 17837
kozick@bucknell.edu

Brian M. Sadler

Army Research Laboratory
Adelphi, MD 20783
bsadler@arl.mil

ABSTRACT

Multiple sensor arrays distributed over a planar region provide the means for highly accurate localization of the (x, y) position of a source. In some applications, such as microphone arrays receiving aeroacoustic signals from ground vehicles, random fluctuations in the air lead to frequency-selective coherence of the signals that arrive at widely separated arrays. We present a performance analysis for localization of a wideband source using multiple sensor arrays. The wavefronts are modeled with perfect spatial coherence over individual arrays and with frequency-selective coherence between distinct arrays. The sensor signals are modeled as wideband Gaussian random processes, and we study the Cramer-Rao bound (CRB) on source localization accuracy for varying levels of signal coherence and for processing schemes with different levels of complexity. We show that significant improvements in source localization accuracy are possible when partial signal coherence from array to array is exploited. Further, we show that a distributed processing scheme involving bearing estimation at the individual arrays and time-delay estimation between pairs of sensors performs nearly as well as the optimum scheme that jointly processes the signals from all sensors. Results based on measured aeroacoustic data are included to illustrate frequency-selective signal coherence at distributed arrays.

1. INTRODUCTION

We are concerned with estimating the location (x_s, y_s) of a wideband source using multiple sensor arrays that are distributed over an area. We consider schemes that distribute the processing between the individual arrays and a fusion center in order to limit the communication bandwidth between arrays and fusion center. Triangulation is a standard approach for source localization with multiple sensor arrays. Each array estimates a bearing and transmits the bearing to the fusion center, which combines the bearings to estimate the source location (x_s, y_s). Triangulation is characterized by low communication bandwidth and low complexity, but it ignores *coherence* that may be present in the wavefronts that are received at distributed arrays. In this paper, we investigate new approaches for source localization with multiple arrays that exploit partial coherence of the wavefronts at distributed arrays. We show that the Cramer-Rao lower bound (CRB) on estimating the source location is significantly reduced when coherence from array to array is exploited. We also evaluate the performance of suboptimum source localization methods that employ distributed processing to reduce the communication bandwidth between the arrays and the fusion center. Results are presented from processing measured aeroacoustic data to illustrate signal coherence at distributed arrays.

Previous work on source localization with aeroacoustic arrays has focused on angle of arrival estimation with a *single* array [1]. The problem of imperfect spatial coherence in the context of narrowband angle-of-arrival estimation with a single array has been studied in [2]-[5]. Pauraj and Kailath [2] presented a MUSIC algorithm that incorporates the nonideal spatial coherence, assuming that the coherence variation is known. Gershman et al. [3] provided a procedure to jointly estimate the spatial coherence loss and the angles of arrival. Song and Ritcey [4] provide maximum-likelihood (ML) methods for estimating the parameters of a coherence model and the angles of arrival, and Wilson [5] incorporates physical models for the spatial coherence. The problem of decentralized array processing has been studied in [6]-[8]. Wax and Kailath [6] present subspace algorithms for narrowband signals and distributed arrays, assuming perfect spatial coherence across each array but neglecting the spatial coherence between arrays. Weinstein [7] presents performance analysis for pairwise processing the wideband sensor signals from a single array and shows negligible loss in localization accuracy when the SNR is high. Stoica, Nehorai, and Soderstrom [8] consider ML angle of arrival estimation with a large, perfectly coherent array that is partitioned into subarrays.

2. DATA MODEL

A model is formulated in this section for the signals received by the sensors in distributed arrays. Consider a single source that is located at coordinates (x_s, y_s) in the (x, y) plane. Then H arrays are distributed in the same plane, as illustrated in Figure 1. The signals measured at the distributed sensor arrays are modeled as jointly Gaussian wideband random processes. The model is very general, and it accounts for propagation effects between the source and the distributed arrays, including frequency-selective spatial coherence and different signal power levels received at each array. The spatial coherence of the wavefronts is modeled as being perfect over each individual array but variable between distinct arrays. This idealization allows us to study the effect of varying coherence between arrays on source localization accuracy. Physical modeling of frequency selective coherence is discussed in [9]. The power spectral density of the source is arbitrary, allowing a range of cases to be modeled including narrowband sources and sums of harmonics, as well as wideband sources with continuous power spectra.

Each array $h \in \{1, \ldots, H\}$ contains N_h sensors, and has a reference sensor located at coordinates (x_h, y_h). The location of sensor $n \in \{1, \ldots, N_h\}$ is at $(x_h + \Delta x_{hn}, y_h + \Delta y_{hn})$, where $(\Delta x_{hn}, \Delta y_{hn})$ is the relative location with respect to the reference sensor. If c is the speed of propagation, then the propagation time from the source to the reference sensor on array h is

$$\tau_h = \frac{r_h}{c} = \frac{1}{c}\left[(x_s - x_h)^2 + (y_s - y_h)^2\right]^{1/2}. \qquad (1)$$

We will assume that the wavefronts are well approximated by plane waves over the aperture of individual arrays. The propagation time from the source to sensor n on array h will be expressed by $\tau_h + \tau_{hn}$, where

$$\begin{aligned} \tau_{hn} &\approx -\frac{1}{c}\left[\frac{x_s - x_h}{r_h}\Delta x_{hn} + \frac{y_s - y_h}{r_h}\Delta y_{hn}\right] \\ &= -\frac{1}{c}\left[(\cos\phi_h)\Delta x_{hn} + (\sin\phi_h)\Delta y_{hn}\right], \qquad (2) \end{aligned}$$

where τ_{hn} is the propagation time from the reference sensor on array h to sensor n on array h, and ϕ_h is the bearing of the source with respect to array h. Note that while the far-field approximation (2) is reasonable over individual array apertures, the wavefront curvature that is inherent in (1) must be retained in order to accurately model the (possibly) wide separation between arrays.

The time signal received at sensor n on array h due to the source will be represented as $s_h(t - \tau_h - \tau_{hn})$, where the vector of signals $\mathbf{s}(t) = [s_1(t), \ldots, s_H(t)]^T$ received at the H arrays are modeled as real-valued, continuous-time, zero-mean, wide-sense stationary, Gaussian random processes with $-\infty < t < \infty$. These processes are fully specified by the $H \times H$ cross-correlation function matrix

$$\mathbf{R}_s(\tau) = E\{\mathbf{s}(t+\tau)\,\mathbf{s}(t)^T\}, \qquad (3)$$

where E denotes expectation, superscript T denotes transpose, and we will later use the notation superscript $*$ and superscript H to denote complex conjugate and conjugate transpose, respectively. The (g, h) element in (3) is the cross-correlation function

$$r_{s,gh}(\tau) = E\{s_g(t+\tau)\,s_h(t)\} \qquad (4)$$

between the signals received at arrays g and h. The correlation functions (3) and (4) are equivalently characterized by their Fourier transforms, which are the cross-spectral density functions and matrix

$$\begin{aligned} G_{s,gh}(\omega) &= \mathcal{F}\{r_{s,gh}(\tau)\} = \int_{-\infty}^{\infty} r_{s,gh}(\tau)\exp(-j\omega\tau)\,d\tau \\ \mathbf{G}_s(\omega) &= \mathcal{F}\{\mathbf{R}_s(\tau)\}. \qquad (5) \end{aligned}$$

The diagonal elements $G_{s,hh}(\omega)$ of (5) are the power spectral density (PSD) functions of the signals $s_h(t)$, and hence they describe the distribution of average signal power with frequency. The model allows the average signal power to vary from one array to another. Indeed, the PSD may even vary from one array to another to reflect propagation differences, source aspect angle differences, and other effects that lead to coherence degradation in the signals at distributed arrays.

Let us elaborate the definition and the meaning of *coherence* between the signals $s_g(t)$ and $s_h(t)$ received at distinct arrays g and h. In general, the cross-spectral density function (5) can be expressed in the form

$$G_{s,gh}(\omega) = \gamma_{s,gh}(\omega)\,\left[G_{s,gg}(\omega)G_{s,hh}(\omega)\right]^{1/2}, \qquad (6)$$

where $\gamma_{s,gh}(\omega)$ is the spectral coherence function, which has the property $0 \leq |\gamma_{s,gh}(\omega)| \leq 1$. The coherence function $\gamma_{s,gh}(\omega)$ is generally complex-valued, but we will model it as real-valued. This is a reasonable assumption for acoustic propagation environments in which the loss of coherence is due to random changes in the apparent source location, as long as the change in apparent source location is the same at both arrays g and h [5, 9].

We model the signal received at sensor n on array h as a sum of the delayed source signal and noise,

$$z_{hn}(t) = s_h(t - \tau_h - \tau_{hn}) + w_{hn}(t), \qquad (7)$$

where the noise signals $w_{hn}(t)$ are modeled as real-valued, continuous-time, zero-mean, wide-sense stationary, Gaussian random processes that are uncorrelated at distinct sensors. The noise correlation properties are

$$E\{w_{gm}(t+\tau)w_{hn}(t)\} = r_w(\tau)\,\delta_{gh}\delta_{mn}, \qquad (8)$$

where $r_w(\tau)$ is the noise autocorrelation function, and the noise power spectral density is $G_w(\omega) = \mathcal{F}\{r_w(\tau)\}$. We then collect the observations at each array h into $N_h \times 1$ vectors $\mathbf{z}_h(t) = [z_{h1}(t), \ldots, z_{h,N_h}(t)]^T$ for $h = 1, \ldots, H$, and we further collect the observations from the H arrays into a $(N_1 + \cdots + N_H) \times 1$ vector

$$\mathbf{Z}(t) = \left[\begin{array}{ccc} \mathbf{z}_1(t)^T & \ldots & \mathbf{z}_H(t)^T \end{array}\right]^T. \qquad (9)$$

The elements of $\mathbf{Z}(t)$ in (9) are zero-mean, wide-sense stationary, Gaussian random processes. We can express the cross-spectral density matrix of $\mathbf{Z}(t)$ in a convenient form with the following definitions. The array manifold for array h at frequency ω is

$$\begin{aligned} \mathbf{a}_h(\omega) &= \begin{bmatrix} \exp(-j\omega\tau_{h1}) \\ \vdots \\ \exp(-j\omega\tau_{h,N_h}) \end{bmatrix} \qquad (10) \\ &= \begin{bmatrix} \exp\left[j\frac{\omega}{c}\left((\cos\phi_h)\Delta x_{h1} + (\sin\phi_h)\Delta y_{h1}\right)\right] \\ \vdots \\ \exp\left[j\frac{\omega}{c}\left((\cos\phi_h)\Delta x_{h,N_h} + (\sin\phi_h)\Delta y_{h,N_h}\right)\right] \end{bmatrix}, \end{aligned}$$

using τ_{hn} from (2) and assuming that the sensors have omnidirectional response to sources in the plane of interest. Let us define the relative time delay of the signal at arrays g and h as $D_{gh} = \tau_g - \tau_h$, where τ_h is defined in (1). Then the cross-spectral density matrix of $\mathbf{Z}(t)$ in (9) has the form

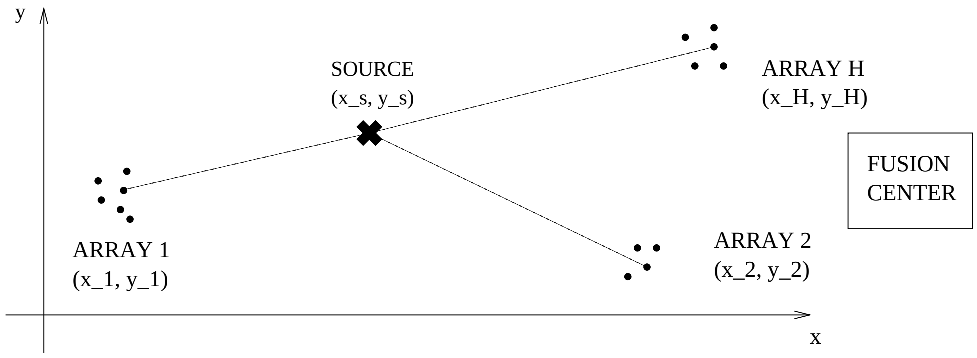

Figure 1: Geometry of source location and H distributed sensor arrays. A communication link is available between each array and the fusion center.

shown in (11) in Figure 2. Recall that the source cross-spectral density functions $G_{s,gh}(\omega)$ in (11) can be expressed in terms of the spectral coherence $\gamma_{s,gh}(\omega)$ using (6).

Note that (11) depends on the source location parameters (x_s, y_s) through $\mathbf{a}_h(\omega)$ and D_{gh}. However, (11) points out that the observations are also characterized by the bearings $\phi_1, \ldots, \phi_H$ to the source from the individual arrays and the relative time delays D_{gh} between pairs of arrays. Therefore, one way to estimate the source location (x_s, y_s) is to first estimate the bearings $\phi_1, \ldots, \phi_H$ and the pairwise time delays D_{gh}.

3. CRBS ON LOCALIZATION ACCURACY

The problem of interest is to estimate the source location parameter vector $\mathbf{\Theta} = [x_s, y_s]^T$ using T samples of the sensor signals $\mathbf{Z}(0), \mathbf{Z}(T_s), \ldots, \mathbf{Z}((T-1)\cdot T_s)$, where T_s is the sampling period. Let us denote the sampling rate by $f_s = 1/T_s$ and $\omega_s = 2\pi f_s$. We will assume that the continuous-time random processes $\mathbf{Z}(t)$ are band-limited, and that the sampling rate f_s is greater than twice the bandwidth of the processes. Then Friedlander [10] has shown that the Fisher information matrix (FIM) $\mathbf{J}$ for the parameters $\mathbf{\Theta}$ based on the samples $\mathbf{Z}(0), \mathbf{Z}(T_s), \ldots, \mathbf{Z}((T-1)\cdot T_s)$ has elements J_{ij} shown in (12) in Figure 2. The CRB matrix $\mathbf{C} = \mathbf{J}^{-1}$ then has the property that the covariance matrix of any unbiased estimator $\hat{\mathbf{\Theta}}$ satisfies $\mathrm{Cov}(\hat{\mathbf{\Theta}}) - \mathbf{C} \geq \mathbf{0}$, where $\geq \mathbf{0}$ means that $\mathrm{Cov}(\hat{\mathbf{\Theta}}) - \mathbf{C}$ is positive semidefinite. The CRB provides a lower bound on the performance of any unbiased estimator. Equation (12) provides a convenient way to compute the FIM for the distributed sensor array model. It provides a powerful tool for evaluating the impact that various parameters have on source localization accuracy. Parameters of interest include the spectral coherence between distributed arrays, the signal bandwidth and power spectrum, the array placement geometry, and the SNR. The FIM in (12) is not easily evaluated analytically, but it is readily evaluated numerically for cases of interest. The FIM expression (12) can be specialized for two important cases. With $H = 2$ arrays containing $N_1 = N_2 = 1$ sensor each, we obtain a generalization of the classic time delay estimation problem [11] with *partial* signal coherence at the sensors. For arbitrary number of arrays H and $N_1, \ldots, N_H$, we can specialize (12) for sources with a *narrowband* power spectrum.

The CRB based on (12) provides a performance bound on source location estimation methods that jointly process all the data from all the sensors. Such processing provides the best attainable results, but it also requires significant communication bandwidth to transmit data from the individual arrays to the fusion center. We have developed performance bounds for schemes that perform bearing estimation at the individual arrays in order to reduce the required communication bandwidth to the fusion center. These CRBs facilitate a study of the tradeoff between source location accuracy and communication bandwidth between the arrays and the fusion center. Two methods are considered [12]:

1. Ordinary triangulation, where each array estimates the source bearing and transmits the bearing estimate to the fusion center. This approach does not exploit wavefront coherence between the distributed arrays, but it minimizes the communication bandwidth between the arrays and the fusion center.
2. Each array estimates the source bearing and transmits the bearing estimate to the fusion center. In addition, the raw data from *one sensor* in each array is transmitted to the fusion center. The fusion center then estimates the propagation time delay between pairs of distributed arrays, and triangulates these time delay estimates with the bearing estimates to localize the source.

Method 2 performs nearly as well as optimum joint processing if the SNR is high enough.

4. EXAMPLES

We present an example that illustrates the potential improvement in source localization accuracy when coherence between the distributed arrays is exploited. Consider a scenario with $H = 3$ arrays, where the individual arrays are identical and contain $N_1 = N_2 = N_3 = 7$ sensors. Each array is circular and has 4-ft radius, with six sensors equally spaced around the perimeter and one sensor in the center. Narrowband processing in a 1-Hz band centered at 50 Hz is assumed, with an SNR of 10 dB at each sensor, i.e., $G_{s,hh}(\omega)/G_w(\omega) = 10$ for $h = 1, \ldots, H$ and $2\pi(49.5) < \omega < 2\pi(50.5)$ rad/sec. The signal coherence $\gamma_{s,gh}(\omega) = \gamma_s(\omega)$ is varied between 0 and 1. We assume that $T = 4000$ time samples are obtained at each sensor with sampling rate $f_s = 2000$ samples/sec. The source localization performance is evaluated by computing the radius of the ellipse in (x, y) coordinates that satisfies the expression $\begin{bmatrix} x & y \end{bmatrix} \mathbf{J} \begin{bmatrix} x \\ y \end{bmatrix} = 1$, where $\mathbf{J}$ is the FIM. If the errors in (x, y) localization are jointly Gaussian distributed, then the ellipse represents the contour at one standard deviation in root-mean-square (RMS) error. The error ellipse for any unbiased estimator of source location cannot be smaller than this ellipse derived from the FIM.

The $H = 3$ arrays are located at coordinates $(x_1, y_1) = (0, 0)$, $(x_2, y_2) = (400, 400)$, $(x_3, y_3) = (100, 0)$, and one source is located at $(x_s, y_s) = (200, 300)$, where the units are meters. Figure 3a shows the ellipse radius for various values of the signal coherence $\gamma_s(\omega)$. Note that a significant improvement in localization accuracy is potentially possible with the small value of coherence $\gamma_s(\omega) = 0.1$, and the CRB gets smaller as the coherence increases. Note also that the localization scheme 2 described above (bearing plus time-delay estimation) may perform as well as the optimum, joint processing scheme.

The CRB results in Figure 3a indicate that even small amounts of signal coherence between widely distributed arrays provide the potential for significant improvement in source localization accuracy. We point out that the CRB results for time-delay estimation in this case are optimistic due to the narrowband model for the observations. With narrowband signals at 50 Hz, the time delays are resolvable only within the interval of one period of $(50\,\mathrm{Hz})^{-1} = 0.02$ sec. The CRB assumes that the ambiguities on the order of 0.02 seconds are resolved by an unbiased estimator. This ambiguity in time-delay estimation can be reduced by exploiting the wideband nature of the signals.

Next we present results from measured aeroacoustic data to illustrate typical values of signal coherence at distributed arrays. The experimental setup is illustrated in Figure 3b, which shows the path of a moving ground vehicle and the locations of four microphone arrays (labeled 1, 3, 4, 5). Each array is circular with $N = 7$ sensors, 4-ft radius, and six sensors equally spaced around the perimeter with one sensor in the center. We focus on the 10 second segment indicated by the $\diamond$'s in Figure 3b. Figure 3c shows the power spectral density (PSD) of the data measured at arrays 1 and 3 during the 10 second segment. Note the dominant harmonic at 40 Hz. Figure 3d shows the estimated coherence between arrays 1 and 3 during the 10 second segment. The coherence is approximately 0.85 at 40 Hz, which demonstrates the presence of significant coherence at widely-separated microphones. Exploiting this coherence has the potential for improved source localization accuracy, as illustrated in the CRBs of Figure 3a. The Doppler effect due to source motion was compensated prior to the coherence estimate shown in Figure 3d.

5. REFERENCES

[1] T. Pham and B. M. Sadler, "Adaptive wideband aeroacoustic array processing," *8th IEEE Statistical Signal and Array Processing Workshop,* pp. 295–298, Corfu, Greece, June 1996.

[2] A. Paulraj and T. Kailath, "Direction of arrival estimation by eigenstructure methods with imperfect spatial coherence of wavefronts," *J. Acoust. Soc. Am.*, vol. 83, pp. 1034-1040, March 1988.

[3] A.B. Gershman, C.F. Mecklenbrauker, J.F. Bohme, "Matrix fitting approach to direction of arrival estimation with imperfect spatial coherence," *IEEE Trans. on Signal Proc.*, vol. 45, no. 7, pp. 1894-1899, July 1997.

[4] B.-G. Song and J.A. Ritcey, "Angle of arrival estimation of plane waves propagating in random media," *J. Acoust. Soc. Am.*, vol. 99, no. 3, pp. 1370-1379, March 1996.

[5] D.K. Wilson, "Performance bounds for acoustic direction-of-arrival arrays operating in atmospheric turbulence," *J. Acoust. Soc. Am.*, vol. 103, no. 3, pp. 1306-1319, March 1998.

[6] M. Wax and T. Kailath, "Decentralized processing in sensor arrays," *IEEE Trans. on Acoustics, Speech, Signal Processing*, vol. ASSP-33, no. 4, pp. 1123-1129, October 1985.

[7] E. Weinstein, "Decentralization of the Gaussian maximum likelihood estimator and its applications to passive array processing," *IEEE Trans. Acoust., Speech, Sig. Proc.*, vol. ASSP-29, no. 5, pp. 945-951, October 1981.

[8] P. Stoica, A. Nehorai, and T. Soderstrom, "Decentralized array processing using the MODE algorithm," *Circuits, Systems, and Signal Processing*, vol. 14, no. 1, 1995, pp. 17-38.

[9] D.K. Wilson, "Atmospheric effects on acoustic arrays: a broad perspective from models," *1999 Meeting of the IRIS Specialty Group on Battlefield Acoustics and Seismics*, Laurel, MD, September 13-15, 1999.

[10] B. Friedlander, "On the Cramer-Rao Bound for Time Delay and Doppler Estimation," *IEEE Trans. on Info. Theory*, vol. IT-30, no. 3, pp. 575-580, May 1984.

[11] G.C. Carter (ed.), *Coherence and Time Delay Estimation* (Selected Reprint Volume), IEEE Press, 1993.

[12] R.J. Kozick and B.M. Sadler, "Source localization with distributed sensor arrays and partial spatial coherence," *SPIE 2000 AeroSense Symp.*, Orlando, FL, April 24-28, 2000.

$$
\mathbf{G}_{\mathbf{Z}}(\omega) = \begin{bmatrix} \mathbf{a}_1(\omega)\mathbf{a}_1(\omega)^H G_{s,11}(\omega) & \cdots & \mathbf{a}_1(\omega)\mathbf{a}_H(\omega)^H \exp(-j\omega D_{1H}) G_{s,1H}(\omega) \\ \vdots & \ddots & \vdots \\ \mathbf{a}_H(\omega)\mathbf{a}_1(\omega)^H \exp(+j\omega D_{1H}) G_{s,1H}(\omega)^* & \cdots & \mathbf{a}_H(\omega)\mathbf{a}_H(\omega)^H G_{s,HH}(\omega) \end{bmatrix} + G_w(\omega)\mathbf{I} \qquad (11)
$$

$$
J_{ij} = \frac{T}{2\omega_s} \int_0^{\omega_s} \mathrm{trace}\left\{ \frac{\partial\, \mathbf{G}_{\mathbf{Z}}(\omega)}{\partial\, \theta_i}\, \mathbf{G}_{\mathbf{Z}}(\omega)^{-1} \frac{\partial\, \mathbf{G}_{\mathbf{Z}}(\omega)}{\partial\, \theta_j}\, \mathbf{G}_{\mathbf{Z}}(\omega)^{-1} \right\} d\omega, \qquad i, j = 1, 2 \qquad (12)
$$

Figure 2: Cross-spectral density matrix $\mathbf{G}_{\mathbf{Z}}(\omega)$ of $\mathbf{Z}(t)$ in (9), and FIM J for parameters $\mathbf{\Theta} = [x_s, y_s]^T$.

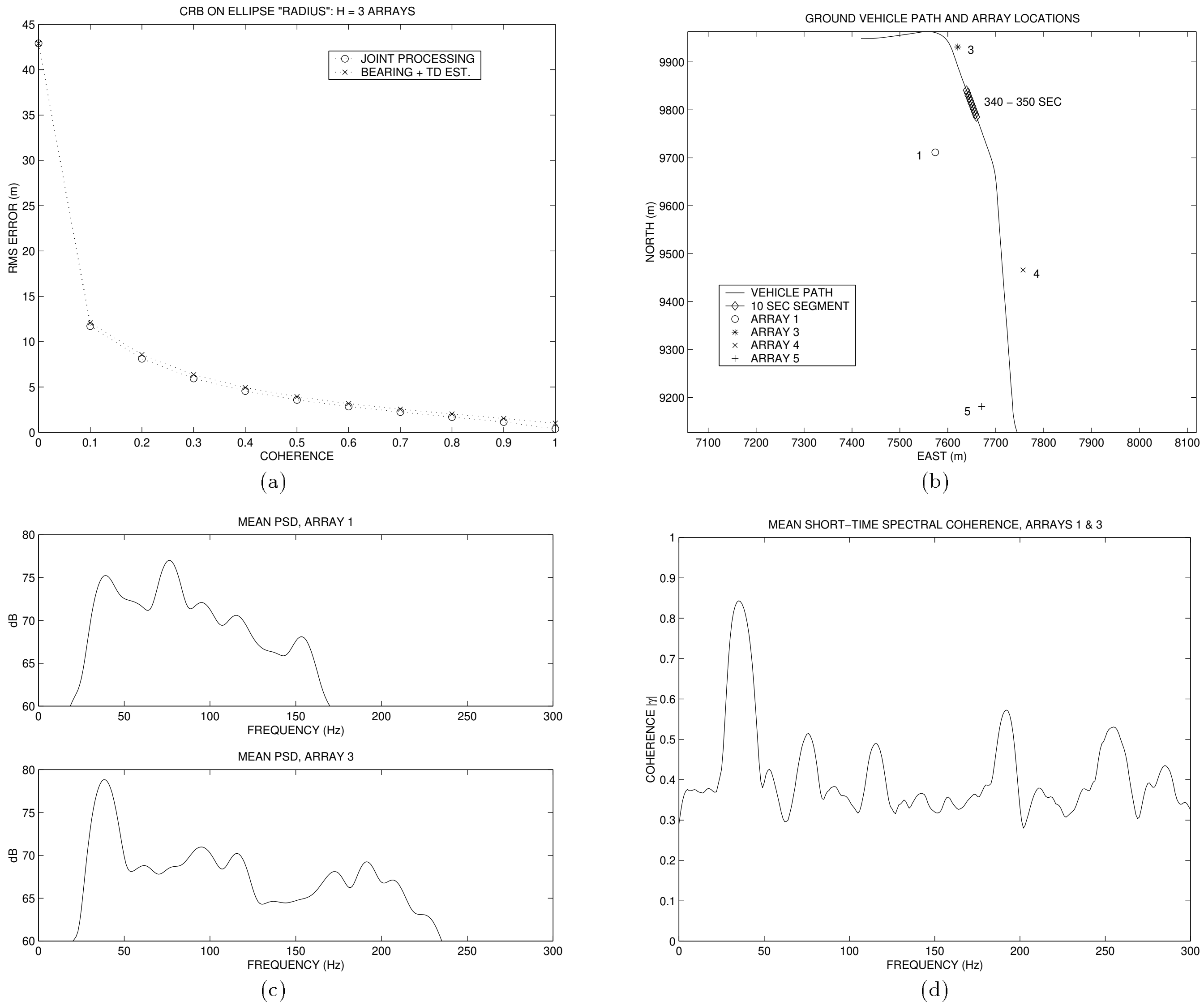

Figure 3: (a) CRBs on RMS source localization error for a scenario with $H = 3$ arrays and one source. (b) Path of ground vehicle and array locations for measured data. (c) Mean power spectral density (PSD) at arrays 1 and 3 estimated from measured data over the 10 second segment $\diamond$ in (b). Top panel is $G_{s,11}(f)$, bottom panel is $G_{s,33}(f)$. (d) Mean spectral coherence $\gamma_{s,13}(f)$ estimated over the 10 second segment.